ISSN (e): **2250 – 3005** || Volume, 07 || Issue, 11|| November – 2017 ||
International Journal of Computational Engineering Research (IJCER)

Piezoelectric-silicone structure for vibration energy harvesting: experimental testing and modelling

[1]MAYURESH MOHARANA, [2]SOAIB AKHTER KHAN,
Gandhi Institute of Excellent Technocrats, Bhubaneswar, India
Bhadrak Institute of Engineering & Technology, Bhadrak, Odisha, India

ABSTRACT:
Mechanical vibrations from heavy machines, building structures, or the human body can be harvested and directly converted into electrical energy. In this paper, the potential to effectively harvest mechanical vibrations and locally generate electrical energy using a novel piezoelectric-rubber composite structure is explored. Piezoelectric lead zirconatetitanate is bonded to silicone rubber to form a cylindrical composite-like energy harvesting device which has the potential to structurally dampen high acceleration forces and generate electrical power.
The device was experimentally load tested and an advanced dynamic model was verified against experimental data. While an experimental output power of 57 µW cm^{-3} was obtained, the advanced model further optimises the device geometry. The proposed energy harvesting device generates sufficient electrical power for structural health monitoring and remote sensing applications, while also providing structural damping for low frequency mechanical vibrations.
Keywords: PZT, silicone, composite, energy harvesting, tube, cylinder, rubber cord

INTRODUCTION

Electricalenergygenerationisparamountinafullyelectrified world powering transport, lighting, computing and health. In order to meet the electrical energy demands, unexplored and abundantlyavailablemechanicalenergycanbeconverteddir- ectly into electrical energy. The harvested electrical energy provides a route for the realisation of autonomous and self- powered, low-power electronic devices [1]. These devices havebeensuccessfullyimplementedaselectromagneticshock absorbers forenergy harvesting [2] or for tire pressuremonitoring [3]. However, when developing energy harvest- ing devices several principles can be applied such as elec- tromagnetic induction [4], triboelectric phenomena [5], or the piezoelectriceffect[6].Thepiezoelectriceffectisofparticular interestbecausepiezoelectricmaterialsdirectlyconvertmech- anical energy into an electric charge when subjected to mech- anicalstress.Ontheotherhand,themostpowerfulpiezoelec- tric materials such as barium titanate oxide ($BaTiO_3$) or lead zirconatetitanate are stiff and brittle ceramics [6] and only a few piezoelectric polymers and co-polymers existinclud- ingpolyvinylidenedifluoride (PVDF) and nylon. Whenusing piezoelectric ceramics various challenges on the device level arise such as, small mechanical designs, material selection and electrical circuits which usually limit the potential of piezoelectric energy harvesting devices. Various mechanical designsexistusingcantileverdesigns[7],bendingdesigns [8] or simply using bulk materials directly for random mechan- icalimpactorcontinuouslowfrequencyvibrations[9].Itis possibletoharvestrandommechanicalimpactfromraindrops [10],trafficinducedbroadbandbridgevibrations[11]ormech- anicalenergyfromhumanmotion[12],withbulkmaterialsor sandwiched structures [13]. However, usually multiple design challenges exist on a device level when tailoring piezoelec- tric materials towards a specific mechanical energy source. For this reason, advanced piezoelectric geometries for spe- cificmechanicalfrequenciesandforcesareincreasinglybeing developed. Examples for advanced piezoelectric geometries arepiezoelectricfibresembeddedintoabi-stablecomposite [14] or woven piezoelectric yarn [15]. Other advanced piezo- electric geometries are ring-type transducers [16] or piezo- electric tubes [17, 18] for structural health monitoring orfluid control [19

$$P=\frac{C}{A} \qquad (1)$$

for the charge density C (C) and material surface area A (A). If the piezoelectric material is exposed to a mechanical force the level of polarisation changes proportionally to the applied mechanical stress. This change in polarisation also leads to a surface effect, where on opposite electrodes electric charge is attracted or repelled by the material's change in polarisa- tion creating an electrical potential difference. This potential difference is available for discharge as an electric voltage. The open-circuit voltage V (V), or electric field E (V m^{-1}), response from a piezoelectric device results from the applied mechanical stress and is defined as[6]:

F d ×t

difficultduetothestiffandbrittlenatureofceramics.For

V=E×t= A ε

(2)

this reason, this paper proposes a piezoelectric tube directly attached to a rubber material as a composite piezoelectric energy harvesting structure. The structure combines powerful piezoelectric ceramics with soft and flexible silicone-rubber creatingapiezoelectricenergyharvestingdevicefromtwodis- similar materials, each with opposing mechanical properties. The combination of high energy harvesting performance in a soft and flexible design provides a novel route to exploiting mechanicalenergyutilisingasimpledevice.Similar,butmore complexdesignedmetalframestructureshavenbeenmodelled [22]. Hence, the silicone-rubber used in the energy harvesting deviceisanidealmaterialforsimplemechanicalmounts(buf- fers, bump stops, bushings) as well as the main component of airinflatedtyres.Inaddition,rubberhasexcellentelasticprop- erties for vibration damping (similar to a mechanical spring) andshieldsobjectsfrommechanicalimpactand/orvibrations, and further provides thermal insulation. Due to the combina- tion of a soft and hard material, the piezoelectric energy har- vesting device combines vibration damping as a passive form of mechanical isolation while continuously generating elec- trical energy from otherwise unused energy from mechanical vibrations.

This paper fully discloses the proposed piezoelectric- silicone structure, provides experimental results of the per- for a given force F (N m^{-1}), area A (m^2), thickness t (m), per- mittivityε (F m^{-1}) and material specific piezoelectric strain coefficient d_{33} (C N^{-1}). The piezoelectric strain coefficient is directional, experiencing strong changes in polarisationparal- lel to the applied mechanical force. When used in an energy harvesting environment with a resistive external electrical load, the generated voltage V from the piezoelectric device determinestheelectriccurrentflowingthroughtheexternal resistiveloadR(Ω)andthecorrespondingpowerasfollows [6]:

$$P = \frac{V^2}{R}. \quad (3)$$

However, since most piezoelectric generatorsexperience vibrations, the mechanical force (F) changes direction intro- ducing alternating currents (AC) through the external load. The generated voltage here can be approximated by the root meansquare(rms)valueforasinusoidalpiezoelectric voltage responseV_{rms}[24].Subsequently,themaximumpowerPfrom thepiezoelectricenergyharvestingdeviceattachedtoares- istiveimpedancematchedexternalelectricloadR_l(Ω)isas follows [25]:

V^2

formance, and validates this using an advanced dynamic modeltooptimisethegeometrytowardsmaximumpowerout- put. Finally, this paper demonstrates a feasible piezoelectric energy harvesting device utilising off-the-shelf components andprovidingaroutetocost-effectiverecoveryofmechanical energy on a smallscale.

with:

$$P_{rms} = \frac{V_{rms}^2}{R_l}$$

$$R_l = \frac{1}{2\times\pi\times f\times C} \quad (4)$$

Methodology

Piezoelectric materials are solid crystal or crystalline mater- ials exhibiting an electric dipole moment or polarisationP (C m^{-2}). The polarisation of piezoelectricmaterials

and source capacitance C (F) of the piezoelectric device. The

capacitance of the piezoelectric device can be approximated in rough analogy to a parallel-plate capacitor with the surface area of the electrodes A, piezoelectric material permittivity ε, and material thickness t as follows:

$$C = \varepsilon\frac{A}{t}. \quad (5)$$

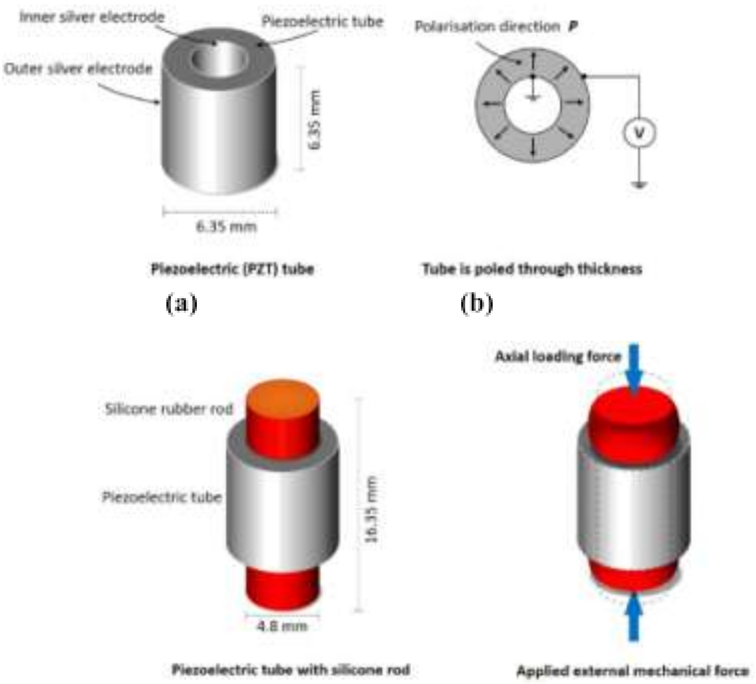

Figure 1. Piezoelectric tube as ring transducers radially polarized across wall thickness (a) and electric circuit connection for voltage signal measurements (b).

According to figure 1, a piezoelectric tube can be radially poled through the wall thickness t with inner and outer elec- trodes. Radially applied mechanical forces then creates the external voltage (V) across the two electrode terminals avail- ablefordischarge.TheemployedpiezoelectricLead(Pb)Zir- conate(Zr)Titanate(Ti)—PZTtubewassourcedfromAPC

(a) **(b)**

Figure 2. Piezoelectric-silicone structure for vibration energy harvesting (a) and visualised under axial mechanical load (b).

perpendicular to the direction of loading. The swelling beha- viourisdefinedforisotopiccylindricalmaterialsbyPoisson's ratio asfollows:
ΔR
in the foreseeable future due to the complex requirements of piezoelectric applications [28]. Hence, when harvesting physical impact with a high mechanical force this ceramic type of piezoelectric material is too hard and too brittle lead- ing to material damage and potentially device failure. In order to overcome this problem, we propose a piezoelectric- silicone rubber cord structure for vibration energy harvest- ing utilizing indirect, or reactive, mechanical forces. For an axial mechanical force, polymeric elastomers can experience

$$\Delta L = \frac{FL}{AE} \quad (6)$$

specificYoung'sModulusE.Accordingtoequation(6),mater- ials with a small Young's Modulus experience large revers- ibledeformations.Largereversibledeformationsalsotranslate into large radial strain deformations, or swelling, ofmaterials for a defined axial strain ΔL and radial strain ΔR.According to equations (6) and (7), materials with a high Poisson'sratio under large compressive forces exhibit large reactive forces in the form of radial strain. This implies the piezoelectric- siliconestructureforvibrationenergyharvestingutilizesindir- ect,orreactive,mechanicalforcesbyswelling.Figure2shows the reversible strain deformation of the piezoelectric-silicone structure under an axial loading force. The reactive swell- ing force of the silicone cord is constrained by the piezo- electric tube transferring mechanical energy onto the piezo- electric tube's inner wall. The piezoelectric tube under force directly exhibits a voltage, utilizing the longitudinal exten- sion mode (3–3) of the piezoelectric-tube, which is avail- able for discharge across an external electric load (equation (3)). In most energy harvesting applications, the quality of the mechanical source energy (force, frequency and acceler- ation) is not adjustable, for which reason the design of energy harvesting devices is limited to mechanical and geometrical optimisations and material selection. Hence, the aim of the analysis is to maximise swelling as a result of external com- pression or axial loading forces. As commercially available piezoelectric tubes are rare and expensive, we optimisedthe length of the silicone cord for maximum swelling and there- foremaximisesecondary,orreactive,mechanicalforcestrans- ferred onto the piezoelectric tube. Due to the complex geo- metryandmaterialmix,itisextremelydifficulttocalculatethe internal force and stress experienced inside the materials and at the interfaces between the silicone-cord and the piezoelec- tric tube. However, in most piezoelectric energy harvesting devicesthemechanicalforce(F)aswellastheelectricfield(E) changes direction necessitating transient analysis. The transi- ent response of the piezoelectric-silicone structure in figure 2can be described by the equation of motion in matrix form as follows[31]:

Table 1. Material properties of piezoelectric-silicone rubber energy harvesting device.

Young's

Relative

Silicone	5	0.470000000	1.3	2.9
PZT	130–150	0.000000031	7500.0	1800.0

for displacement x, mass matrix M, D and K, and electric charge$q$ (C). Due to the continuously changing mechanical force, the complex structure in figure 2(b) exhibits adynamic response with complex vibration modes and resonance. Thus, the proposed experiment compares direct measurements with numerical finite element modelling (FEM) results for gener- atedpowerandavailableenergyundervarioustransientforces.

3. Dynamic testing

This paper reports on dynamic testing of piezoelectric energy harvesting devices under controlled laboratory test condi- tions, in order to approximate energy harvesting performance under real world conditions. While most accelerations, such as human walking, are below 10 g [32], forced accelerations in tyres can reach up to 5000 g [33]. Since representative nat-

u
] [ ]
F
= (8)

Material
Modulus
(GPa) Poisson ratio(–)
Density (kg m^{-3})
permittivity (C m^{-2})

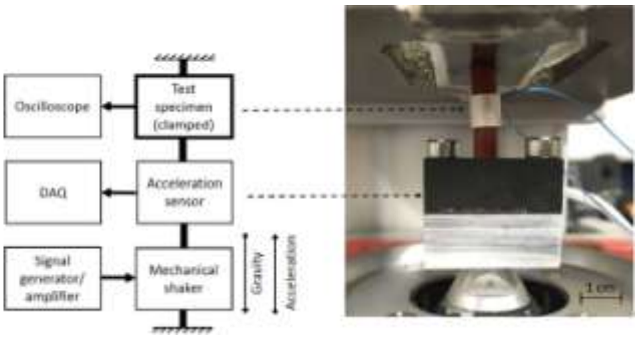

(a) **(b)**

Figure 3. Energy harvesting test set-up equivalent diagram (a) with signal flow direction indicated by arrows and mechanical links illustrated by solid lines. The picture (b) shows a vertical orientated clamped energy harvesting device.

ural accelerations and vibrations are challenging to re-create, thispaperutilisedconstantaccelerationsandcontinuousvibra- tion sources below 50 Hz in order to describe a reproducible energy harvesting set-up and realistically test energy harvest- ingdevices[34].Vibrationsbelow50Hzusuallycoincidewith low acceleration levels around 2–3 g for example in human walking[35].Accordingtofigure3,asignalgeneratorisdriv- ing a sinusoidal voltage into an LDS PA25E power amplifier which supplies power to a mechanical shaker V201-M4-CE. The excitation of the mechanical shaker creates an axialforce actingatthetwoendsurfacesofacylindricalclampedsilicone rubbercordorpiezoelectric-siliconeenergyharvestingdevice. The piezoelectric-silicone device is mechanically load tested under a constant acceleration magnitude of 1 g and 2 g tocre- atecontrolledstructuralforcesanddeformations.Basedonthe reactiveradialstrain(equation(7))thepiezoelectrictubeopen circuitvoltageisdirectlymeasuredbyahighinputimpedance oscilloscopeprobeset- upwithasamplingrateof50MHz.The acceleration excitation was measured using a 10 g accelero- meter data acquisition device with a sampling rate of 10 kHz maintaining 1 g and 2 g excitation acceleration throughout the test. The device was tested at slow frequencies between 10 and 50 Hz while the experimental data was continuously recorded over a minimum of six cycles with a combined cal- culated error for the peak-to-peak voltage (V_{pp}) of 10% at 1 g and 2 g acceleration levels. Following Newton's second law of motion the applied force is maintained constant across all frequency measurements by adjusting the acceleration at the shaker. The shaker was operating parallel to the earth's gravitational force in order to avoid double impact and radial forces on the test specimen. According to table 1, the tested piezoelectric-silicone rubber energy harvesting device shows considerable differences between the employed silicone rub- ber cord and the PZT tube. The silicone cord is made of 95% silicone rubber compound, 2% organic peroxide mixture, 2% ironoxide,and0.5%organopolysiloxane,andsourcedfrom SealmastersLtd(UK)[36].ThePoisson'sratioofthesilicone rubber cord is eight orders of magnitude greater than that of the PZT, indicating its greater flexibility. The Young's modu- lus of 130–150 GPa for PZT indicates very hard mechanical properties compared to 5 MPa of silicone rubber indicating verylightandsoftproperties[37].Theassemblyofthesesub- stantially different materials in a piezoelectric-silicone struc- ture requires the experiment to be reproducible and simple in ordertoderivetheenergyharvestingcapabilitiesofthedevice tested. For this reason, the proposed materials were tested at roomtemperatureaccountingfortheCuriepointofPZTbelow 300˚C[26]andthetransitiontemperatureforsiliconeofover 400˚C[38].Thisleavessufficientspaceforenergyharvesting applications at elevated temperatures, which could be evalu- ated in subsequent studies.

4. Finite elementmodel

An advanced FEM model was developed using elastic ele- ments based on the basic law of motion and coupled with the reactive forces of piezoelectric theory. Due to the high level of directional non-linearity with piezoelectric materi- als, the coupled-field, harmonic and transient response ana- lysiswascarriedoutinANSYSParametricDesignLanguage. The analysis in ANSYS allows for optimisation of the mech- anical design and the material selection. The ANSYS model is comprised of two different volumes representing the pro- posed piezoelectric-silicone rubber energy harvesting device. Based on the material properties in table 1, the first volumeis acylindricalsilicone-rubbercordmeshedinSolid186,bonded

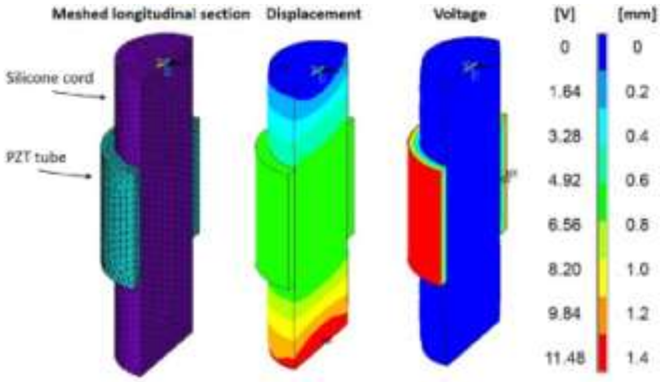

Figure 4. Meshed piezoelectric-silicone longitudinal-section three-dimensional model in ANSYS (colours represent displacement and voltage under mechanical load).

to a second piezoelectric PZT tube-shape volume, meshed in Solid227.ThecommercialFEMsolversfacilitatetheanalysis of the rotational, symmetrical, cylindrical structure by trans- forming the piezoelectric compliance matrix from a geomet- rical Cartesian (x, y, z) system into a geometrical cylindrical (r, θ, z) coordinate system, where the direction of polarization P is taken to be parallel to the radial direction r, or equivalent to axis 3 in the Cartesian coordinates.

withradiusr,angularcoordinateϑ,andcylinderheightz.The silicone-tube cord and piezoelectric tube model exhibits lon- gitudinal (w) and radial (u) displacement and stress while tor- sion is constrained (v). Hence, a structural harmonic analysis, at constant excitation forces (F) for 1 g and 2 g acceleration levels,wasconductedbasedonthefollowingboundarycondi- tions as inputparameters:

u(r),v(ϑ),w(z)=displacementinspace(10)

with:

u(r) = free;

v(ϑ) = 0;

$w(z) = F \times \sin(2 \times \pi \times f);$

for sinusoidal drive frequencies between 10 and 50 Hz and

open circuit piezoelectric voltage. With the longitudinal (z), radial (r), and electrical (E_r) degree of freedom, the vibration modes and resonance frequencies are computed in ANSYS. Due to the relatively low frequency applied in the experi- ment,thedissipationenergyforcyclingstrainloadsinsidethe material was neglected in the model because no temperature changes were observed during the experiments. In addition, hyperplastic effects and/or viscoelastic effects were also neg- lected in the model for simplicity. The direction of polariza- tion is taken to be parallel to the z or axis 3 in the Cartesian coordinate description of piezo-ceramic geometry.

The transformed piezoelectric matrix acts together with the compliance matrix, along with the applied cylindrical loads, inthecylindricalcoordinatesystem,whichprovidesthepiezo- electric voltage based on the experiencedstrain.

Figure 4illustrates, the three-dimensional piezoelectric- silicone energy harvesting structure that was modelledin ANSYSasalongitudinal-sectionoffigure2.Thelongitudinal- section model enables the analysis of the mechanical prin- ciples inside the silicone cord revealing the stress and strain distribution inside the material which is significantly more difficult to physically analyse. Subsequently, the model piezoelectric-silicone rubber device dimensions (figure 2) are optimisedtowardsamaximumopencircuitvoltageforavari- able silicone-rubber cord length asfollows:

V_{pp} (L)=max. (13) Forashortsilicone-rubbercordlength,theswellingforceis concentratedalongthecentreofthepiezoelectrictubeandless sotowardstheunconstrainededges.Foreverychangeinstress concentration,thecomputedvoltageisthenextractedandval- idated against experimental data. Then a longitudinal-section stress analysis is conducted in order to determinemechanical

RESULTS AND DISCUSSIONS

The disclosed piezoelectric energy harvesting device was bench tested and the FEM model was verified against the obtained experimental data. generates an open circuit voltage peak-to- peak V_{pp}(V) of 11.5 V at 10 Hz driving frequency and 1 g excitation acceleration ($E_r$in equation (10)).

When doubling

$$[c] = \begin{bmatrix} 12.7 & 8.0 & 8.5 & 0 & 0 & 0 \\ & 12.7 & 8.5 & 0 & 0 & 0 \\ & & 11.7 & 0 & 0 & 0 \\ & & & 2.3 & 0 & 0 \\ & & & & 2.3 & 0 \\ & & & & & 2.4 \end{bmatrix} . \quad (12)$$

the excitation acceleration to 2 g at 10 Hz the open circuit voltage nearly doubles to 21.0 V. This loosely linear relation- ship between open circuit voltage and acceleration excitation was present for driving frequencies of up to 30 Hz. At 30 Hz the open circuit voltage at 1 g is 3.3 V and 6.4 V at 2 g. For higher frequencies over 30 Hz the measured opencircuit

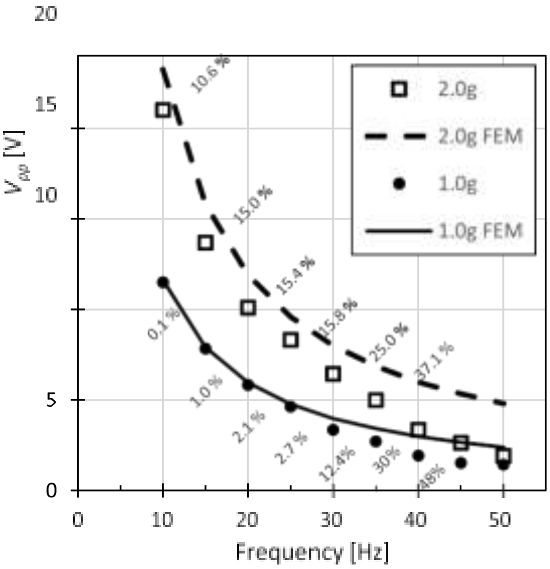

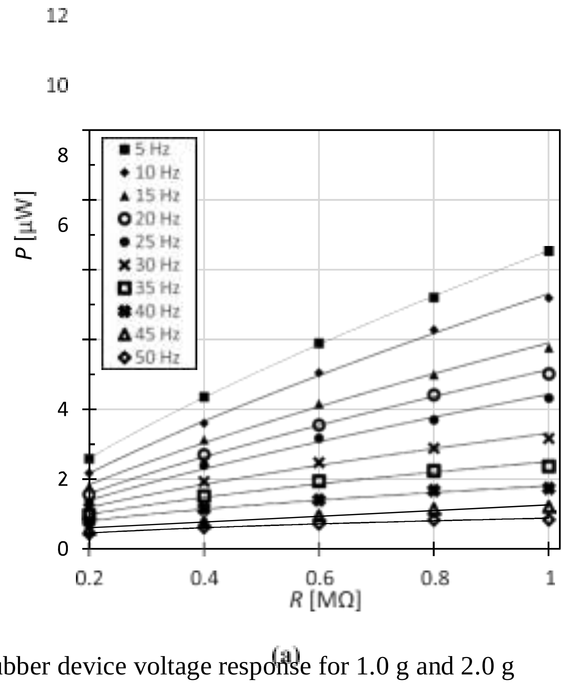

Figure 5. Peak-to-peak open circuit piezoelectric-silicone rubber device voltage response for 1.0 g and 2.0 g excitation acceleration (indicating the FEM error in %).

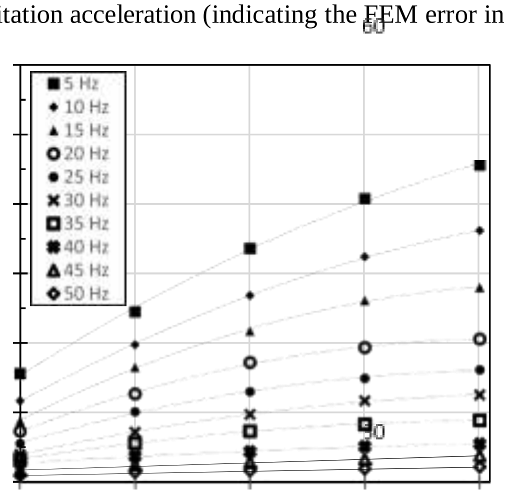

voltage is no longer proportional to the increases in accelera- tionexcitationandthedeviceonlygeneratesavoltageof1.9V at2gcomparedto1.4Vat1gat50Hz.TheFEMmodelcon- sistentlyoverestimatedthepeakvoltagewithanerrorofupto 2.7%atfrequenciesbelow30Hzat1gandupto15.8%atfre- quenciesbelow35Hzat2g.Theerrorisindicatedinfigure5. For the measured open circuit voltage in figure 5, it is pos- sible to calculate the available power of the energy harvesting device (equation(4)).

According to equation (4), the optimal load resistance is a function of the driving frequency. Subsequently, the optimal resistancesfortheinvestigatedfrequencyrangearebetween
6.37 MΩ (at 10 Hz) and 1.27 MΩ (at 50 Hz). However,since
piezoelectricACishardlyusedinpracticalenergyharvest-
ing applications external rectifier circuits are necessary [40].
of8.5µWisdissipatedat5Hzand1MΩ.Accordingto
equation(3),thedissipatedpowerPforlowerexternalload
resistancesR and higher frequencies appears to decrease lin- early.However,at2ginfigure6(b)apowerof45.4µWis dissipated at 5 Hz and 1 MΩ and decreases for smallerresist-
ances.Thedissipatedpoweralsodecreasesforhigherfrequen-
cies since the duration of the force is shorter (equation (2)).

Figure 7shows a calculated, and impedance matched (equation(4)),P_{rms}poweroutputof86.5µW(specificenergy densityof57µWcm^{-3})obtainedat2gaccelerationexcitation andatthelowestfrequencymeasuredof10Hz.DuetotheAC characteristics of the piezoelectric energy harvesting device theaverageP_{rms}inequation(4)providesareasonableestimate

100
40
80
R [MΩ]
(b)
60
P [μW]

of open-circuits voltage improvements for the energy harvesting device performance. However, for increasing drive frequencies the power gains resulting from thevoltageimprovementsdiminishslowly.At50Hztheaver- age power at 1 g is 2 μW compared to 3.6 μW at 2 g, indic- ating that the proposed device is more suited towards lowfre- quenciesandhighaccelerationexcitation.Themeasuredopen circuit voltage is compared with the calculated open circuit voltageoftheFEMmodelinfigure5.Thecalculatedopencir- cuitvoltagehasareasonableaccuracyatlowexcitationaccel- erationandfrequenciesbelow25Hz.However,thecalculated voltageresponseof5Vat50Hzand1gissignificantlyhigher

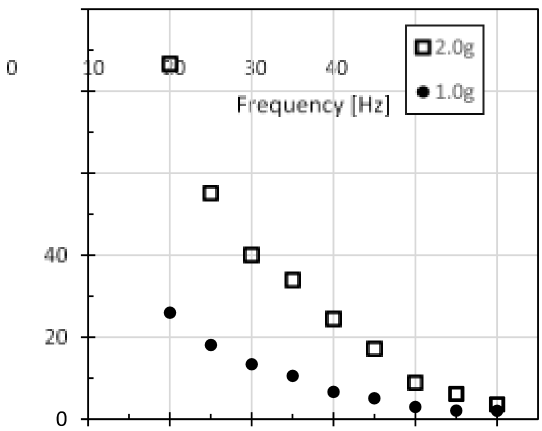

Figure 7. Peak power of piezoelectric-silicone rubber device voltage response for 1.0 g and 2.0 g excitation acceleration.

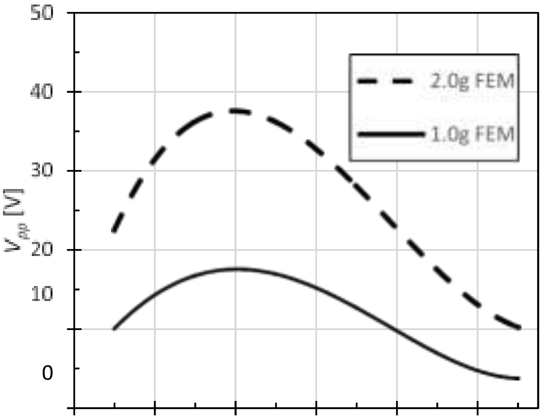

Figure 8.FEM optimised peak-voltage of piezoelectric-silicone rubber as a function of silicone rubber length at 10 Hz drive frequency for 1 g and 2 g excitation acceleration.

than the experimental voltage response of 1.92 V. Hence, the conductedFEMmodelgraduallylosesaccuracywithincreas- ing frequencies and accelerations. A lack of viscoelastic and heating effects in the FEM model potentially leads to a dis- crepancy between measured open circuit voltage in theexper- iment and computed open circuit voltage in the FEM model. Theseeffectsaremorelikelytonegativelyaffectasoftmater- iallikerubberintheexaminedhighfrequencyenergyharvest- ing environment, compared to a hard piezoelectric ceramic (table 1). In addition, the calculated harmonic and transient response of the model potentially includes complex dynamic changes within the energy harvesting device. Hence, the pro- posedmodelprovidesagoodreferenceforlowfrequency and low excitation acceleration applications and optimisations. In order to optimise the device performance at low frequencies and low excitation accelerations the effect of silicone-cord length on the design needs to be analysed (equation (12)). The length of the silicone cord is optimised based on thebest

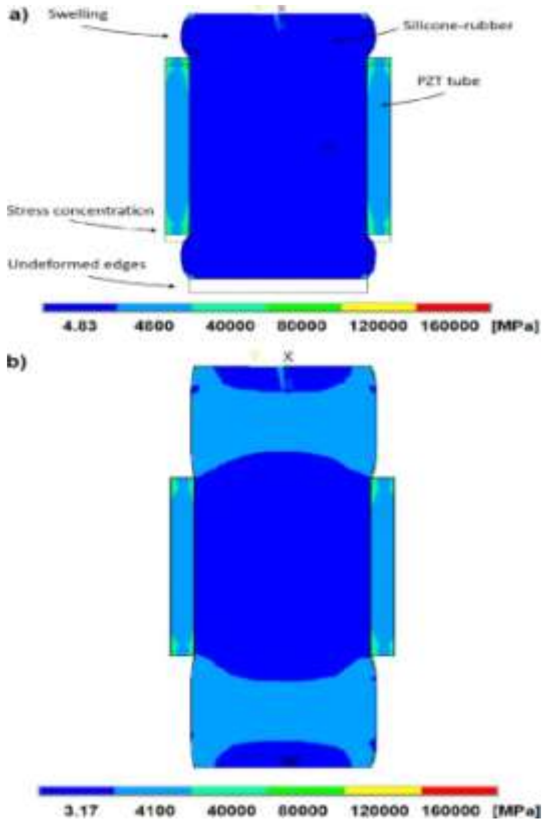

Figure 9.FEM stress analysis for a 10 mm (a) and 15 mm (b) silicone rubber cord length at 1 g and 10 Hz with stress concentrated at the piezoelectric tube edges.

possibleFEMmodelaccuracyat10Hzfor1gand2g.Accord- ing to figure 7, the peak open circuit voltage of the energy harvesting device is seen for a 13 mm silicone cord length with a maximum voltage of 17.6 V. At 2 g excitation acceler- ation, the maximum open circuit voltage is 38 V for the same 13mmsilicone-cordlength.Accordingtofigure8,theoptimal length of the silicone-cord for 1 g and 2 g of excitation is 13 mm with rapidly decreasing performance for shorter and longer silicone-cord lengths. For higher excitation levels the peak voltage flattens out more rapidly than for lower excita- tion levels. For short cord lengths below 13 mm, this highly non-linear performance is limited by the swelling area of the silicone cord. Below 10 mm, axial forces on the piezoelectric tubearehigherthantheappliedradialforces,creatingelectric fields perpendicular to the electrodes ($E_z$in equation(10)).

Figure 9(a) shows a FEM mechanical stress analysis for a 10 mm silicone rubber cord length longitudinal-section at 1 g and 10 Hz with high stress concentrations at the piezoelectric tubeedges(figure4).Thecolourbarindicatesahomogeneous

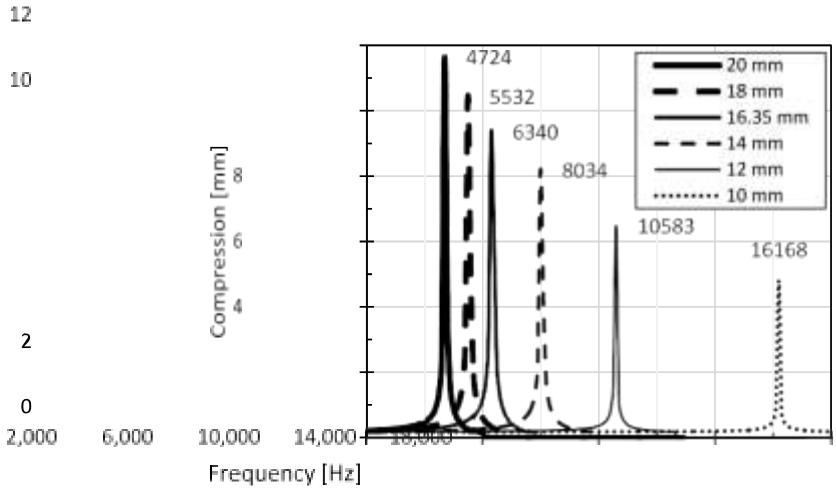

Figure 10. First mode harmonic simulation compression of various piezoelectric-silicone device lengths at 1 g.

stress level across the silicone-rubber of 4.83 MPa which is close to the material limit of 5 MPa. Compared to the unde- formed material edges, substantial swelling is present where the silicone-cord is unconstrained by the piezoelectric tube. However, the piezoelectric tube experiences substantial stress at the tube edges due to non-uniform loading effects from the swelling rubber close to the mechanical limit (table 1). Com- pared to a 15 mm long silicone cord figure 9(b), the swell- ingbehaviour is less apparent because the mechanical load is distributed across a greater volume, with stress concentrated in unconstrained areas. The cord length of 10 mm represents thedesignlimitofthesilicone-rubber,whichisdeterminedby theYoung's Modulus.MaterialswithagreaterYoung'sModu- lusandequallyhighPoisson'sratiocouldpotentiallyimprove the energy harvesting performance of the device. Despite the greater strain deformation of the 15 mm cord (figure 9(b)), comparedtothe10mmcord(figure9(a)),themodelleddevice under clamped conditions exhibits a linear increase in max- imum displacement for increasing silicone-cord lengths by a factor of 0.046 at 10 Hz and 1g

Figure 10compares the first mode harmonic simulation displacement response for 10, 12, 14, 16.35, 18, and 20 mm silicone rubber cord length devices at 1 g. Beyond the fre- quency range of experimental interest, the devices experience high displacement at resonance frequency (f_r). The 20 mm long cord device exhibits a maximum excitation of 11.6 mm ataresonancefrequencyof4724Hz.Theresonancefrequency increasesforshortercorddevicesto5532Hzfora18mmcord and 6340 Hz for a 16.35 mm cord (figure 2(b)). When com- pared to long cord devices, short cords experience a signific- antlyhigherresonancefrequency.The10mmlongdevicehas a resonance frequency of 16,168 Hz. Thus, the silicone-cord length can be considered a mechanism to shift the resonance frequency.

Consequently, the proposed energy harvesting structure can harvest mechanical energy at maximum displacement, potentially leading to a higher energy yield [43]. On the other hand, the compression of the silicone rubber at resonance frequency exceeds the maximum value of 35% for all cord lengths,potentiallyleadingtomechanicalfailureoftheenergy harvestingdevice[35].Accordingtothefrequencyresponseof the piezoelectric-silicone device in figure 10, the correspond- ingmechanicaldampingratioisderivedforthesiliconerubber cord based on the half-power frequency response magnitude. With a damping ratio of 0.06 at resonance for all silicone rod lengths, the energy harvesting devices exhibit an elastic fre- quencyresponseandaqualityfactorof8.3whichiswithinthe range for rubber structures [44]. Hence, the mechanical prop- erties of the silicone cord are similar to pure silicone rubber and are not compromised by the piezoelectric tube.

CONCLUSIONS

Due to the volatile nature of electricity and the limited abil- ity of storing electrical energy, it is challenging to implement changes and improvements to energy efficiency, conver- sion effectiveness and generator size and weight. However, the proposed piezoelectric-silicone rubber energy harvesting device effectively generates electrical energy from mechan- icalenergy. The performance is primarily determined by the design (shape, size, material selection) and external factors (mechanical excitation amplitude, frequency). When optim- ising the design, materials with a high Poisson's ratio are favourable while the piezoelectric materials with a high piezoelectric coefficient (i.e. ceramics) are preferred.Other approaches may be possible with piezoelectric polymers. The proposedrelativeoptimisationmethodcomparesthelength of the silicone-cord to the open circuit voltage. The results show that off-the-shelf FEM models overestimate the device per- formance and do not accurately reproduce the complexity of the electro-mechanical interaction. Finally, the complexity of themulti-physicsenergyharvestingdevicewithmaterialprop- erties spreading across several orders of magnitude requires a careful experimental optimisation due to the material mixand secondaryphysicaleffects.Futureexperimentalworkwilltar- get an embedded piezoelectric tube structure for compression and elongation energy harvesting while numerical work will targetthedevelopmentofacustom-builtFEMsolver,address- ingallunderlyingphysicalprinciplesofthedevice.Despitethe successful proof-of-concept of a highly flexible energy har- vesting device, the idea of harvesting the world's mechanical energy with piezoelectric materials is still a significant chal- lenge.

REFERENCES

[1] Liu H, Fu H, Sun L, Lee C and YeatmanE M 2020 Hybrid energy harvesting technology: from materials, structural design, system integration to applications Renew.Sustain.Energy Rev. **137** 110473

[2] Li Z, Zuo L, Luhrs G, Lin L and Qin Y X 2012 Electromagnetic energy-harvesting shock absorbers:design, modeling, and road tests IEEE Trans. Veh.Technol.**62**1065–74

[3] Bowen C R and Arafa M H 2015 Energy harvesting technologies for tire pressure monitoring systemsAdv.Energy Mater.**5**1401787

[4] Yang B, Lee C, Xiang W, Xie J, He J H, Kotlanka R K, Low S P and Feng H 2009 Electromagnetic energy harvesting from vibrations of multiple frequenciesJ.Micromech.Microeng.**19**035001

[5] Wang S, Lin L and Wang Z L 2015 Triboelectricnanogenerators as self-powered active sensors Nano Energy**11**436–62

[6] Bowen C R, Kim H A, Weaver P M and Dunn S 2014 Piezoelectric and ferroelectric materials and structures for energy harvesting applications Energy Environ.Sci.**7**25–44

[7] Sharpes N, Abdelkefi A and Priya S 2014 Comparative analysis of one-dimensional and two-dimensional cantilever piezoelectric energy harvesters Energy HarvestingSyst.**1**209–16

[8] Harris P, Skinner W, Bowen C R and Kim H A 2015 Manufacture and characterisation of piezoelectric broadband energy harvesters based on asymmetricbistable cantilever laminates Ferroelectrics **480**67–76

[9] Wang H, Mao M, Liu Y, Qin H, Zhang M and Zhao W 2019 Impact energy harvesting system using mechanical vibration frequency stabilizer Smart Mater.Struct.**28**075006

[10] Ilyas M A and Swingler J 2015 Piezoelectric energy harvesting from raindrop impacts Energy **90**796–806

[11] Peigney M and Siegert D 2013 Piezoelectric energy harvesting from traffic-induced bridge vibrations Smart Mater. Struct.**22**095019

[12] QianF, Xu T B and Zuo L 2019 Material equivalence, modeling and experimental validation of a piezoelectricboot energy harvester Smart Mater. Struct. **28**075018

[13] Zhao J and You Z 2014 A shoe-embedded piezoelectric energyharvester for wearable sensors Sensors**14**12497–510

[14] Ji S H, Cho Y S and Yun J S 2019 Wearable core-shell piezoelectric nanofiber yarns for body movement energyharvesting Nanomaterials**9**555

[15] Huan Q, Chen M and Li F 2019 A practical omni-directional SH wave transducer for structural health monitoring based on two thickness-poled piezoelectric half-rings Ultrasonics**94**342–9

[16] Qu J, Huang S, XuY, Jiao H, Xu D and Cheng X 2014 Fabrication and properties of PZT piezoelectric ceramic tubes with large length–diameter ratio Ceram.Int.**40**13019–24

[17] Gao Y H, Jiang S N, Zhu D B and Gao H T 2017 Theoretical analysis of a piezoelectric ceramic tube polarized tangentially for hydraulic vibration energy harvestingArch.Appl. Mech. **87** 607–15

[18] Peelamedu S M, Kosaraju C B, Dukkipati R V and Naganathan N G 2000 Numerical approach for axisymmetric piezoceramic geometries towards fluid control applications Proc. Inst. Mech. Eng. I **214**87–97

[19] Li X, Chuang K and Tzou H 2010 Energy harvesting using a circular cylindrical shell laminated with a segmented piezoelectric layer Proc. 2010 Symp. Piezoelectricity, Acoustic Waves and Device Applications pp139–44

[20] Gencoglu C and Özgüven H N 2014 Optimal placement of piezoelectric patches on a cylindrical shell for active vibration control Topics in Modal Analysis vol 7(Berlin:Springer) pp 673–81

[21] Evans M, Tang L and Aw K C 2018 Modelling and optimisation of a force amplification energy harvesterJ.Intell.Mater. Syst. Struct. **29** 1941–52

[22] Nye J F 1985 Physical Properties of Crystals: Their Representation by Tensors and Matrices (Oxford : OxfordUniversityPress)

[23] Erturk A and Inman D J 2011 Piezoelectric EnergyHarvesting(New York: Wiley)

[24] Kong N A, Ha D S, Erturk A and Inman D J 2010 Resistive impedance matching circuit for piezoelectric energy harvesting J. Intell. Mater. Syst. Struct. **21**1293–302

[25] (Available at: www.americanpiezo.com) (Accessed 28June2020)

[26] Uchino K 2009 Ferroelectric Devices (Boca Raton, FL:CRCPress)

[27] Bell and Deubzer 2018 Lead-free piezoelectrics—the environmental and regulatory issues MRS Bull. **43**581–87

[28] Cao P F et al 2018 Superstretchable, self-healing polymeric elastomers with tunable properties Adv. Funct. Mater. **28**1800741

[29] Beer F P, Johnston E R and DeWolfJ T 1999 Mechanics of Materials 5th SI edn (New York: McGraw-HillEducation)

[30] Xiang H J, Zhang Z W, Shi Z F and Li H 2018 Reduced-order modeling of piezoelectric energy harvesters with nonlinear circuits under complex conditions Smart Mater.Struct.**27**045004

[31] Hoffmann D, Folkmer B and Manoli Y 2013 Human motion energy harvester for biometric data monitoring J.Phys.:Conf. Ser**476**012103

[32] Löhndorf M, KvisterøyT, Westby E and Halvorsen E 2007 Evaluation of energy harvesting concepts for tirepressure monitoring systems Proc. Power MEMS pp331–4

[33] Maamer B, Boughamoura A, El-Bab A M F, Francis L A and TounsiF 2019 A review on design improvements and techniques for mechanical energy harvesting using piezoelectric and electromagnetic schemes EnergyConvers.Manage. **199**111973

[34] Li H, Tian C and Deng Z D 2014 Energy harvesting from low frequency applications using piezoelectric materialsAppl.Phys. Rev. **1**041301

[35] (Available at: www.sealmasters.co.uk/) (Accessed 28June2020)
[36] FettT, Munz D and Thun G 2002 Young's modulus of soft PZT from partial unloading tests Ferroelectrics **274**67–81
[37] Zhang C, Pal K, Byeon J U, Han S M and Kim J K 2011 A study on mechanical and thermal properties of silicone rubber/EPDM damping materials J. Appl. Polym. Sci.**119**2737–41
[38] Burianova L, Bowen C R, Prokopova M and Sulc M2005 Laser interferometric displacement measurements of multi-layer actuators and PZT ceramics Ferroelectrics**320**161–9
[39] Dell'AnnaF, Dong T, Li P, Wen Y, Yang Z, Casu M R, Azadmehr M and Berg Y 2018 State-of-the-art power management circuits for piezoelectric energy harvestersIEEE Circuits Syst. Mag. **18**27–48
[40] KashiwaoT, Izadgoshasb I, Lim Y Y and Deguchi M 2016 Optimization of rectifier circuits for a vibration energy harvesting system using a macro-fiber composite piezoelectric element Microelectron. J. **54**109–15
[41] Liao Y and Liang J 2018 Maximum power, optimal load, and impedance analysis of piezoelectric vibration energy harvesters Smart Mater. Struct. **27**075053
[42] Song H C, Kim S W, Kim H S, Lee D G, Kang CY andNahm S 2020 Piezoelectric energy harvesting des principles for materials and structures: material figure- of- merit and self-resonance tuning Adv. Mater. **32**2002208
[43] BalasubramanianP, Ferrari G and Amabili M 2018 Identification of the viscoelastic response andnonlineardamping of a rubber plate in nonlinear vibration regimeMech. Syst. Signal Process.**111**376–98
[44] BettsDN,KimHA,BowenCRandInmanDJ2012Optimal configurations of bistablepiezo-composites for energy harvesting Appl. Phys. Lett. **100**114104